tion of the charge state of the incident projectile. From comparisons of σ_x in the gas and in the solid, the mean charge of Ar is found to be ~ 11. In this analysis $\bar{\omega}$ is implicitly assumed to be the same in the gas and the solid. In this paper it is shown that $\bar{\omega}$ can change by a factor of 2 since Cl and Ar projectiles are expected to produce similar amounts of multiple ionization. Adjusting the data for the factor of 2 change in $\bar{\omega}$, the mean charge of Ar in the foil is ~ 14 which agrees with the mean charge measured emerging from the solid.

In summary, we have observed a shift in energy and a change in relative intensities of the Si-$K\alpha$ satellite peaks from gas and solid targets when bombarded by 45-MeV Cl ions. The shift of the satellites to higher energy in the gas is attributed to removal of all of the M-shell electrons during the collision. The change in relative intensities between the gas and the solid cannot be explained in terms of L-shell filling by M-shell electrons if single-hole rates are used. Unless better estimates of these rates are much greater than the present values, the amount of multiple L-shell ionization created in the collision is greater in the gas target than in the solid. Both effects will produce a higher $\bar{\omega}$ in the gas than in the solid, which can affect interpretations of low-resolution cross-section data.

The authors would like to thank Jim Hall and Clarence Annett for their assistance in the data acquisition.

*On leave from North Texas State University, Denton, Texas.

†Supported in part by the U. S. Energy Research and Development Administration under Contract No. AT(11-1)-2130.

[1]R. L. Kauffman, C. W. Woods, K. A. Jamison, and P. Richard, Phys. Rev. A 11, 872 (1975).

[2]For example, see P. Richard, in *Atomic Inner-Shell Processes*, edited by B. Crasemann (Academic, New York, 1975), Vol. 1, p. 73.

[3]S. Datz, B. R. Appleton, J. R. Mowat, R. Laubert, R. S. Peterson, R. S. Thoe, and I. A. Sellin, Phys. Rev. Lett. 33, 733 (1974).

[4]Applied Research Labs, Glendale, California.

[5]J. McWherter, D. K. Olsen, H. H. Wolter, and C. F. Moore, Phys. Rev. A 10, 200 (1974).

[6]C. Froese Fischer, Comput. Phys. Commun. 4, 107 (1972).

[7]J. A. Bearden, Rev. Mod. Phys. 39, 78 (1967).

[8]H. D. Betz, Rev. Mod, Phys. 44, 465 (1972); A. B. Wittkower and H. D. Betz, At. Data 5, 113 (1973).

[9]J. E. Bolger, B. M. Johnson, K. S. Roberts, and C. F. Moore, in *Electronic and Atomic Collisions, Abstracts of Papers of the Ninth International Conference on the Physics of Electronic and Atomic Collisions*, edited by J. S. Risley and R. Geballe (Univ. of Washington Press, Seattle, Wash., 1975), Vol. 1, pp. 423–424.

[10]H. R. Philipp and H. Ehrenreich, Phys. Rev. 129, 1550 (1963).

[11]D. L. Walters and C. P. Bhalla, Phys. Rev. A 3, 1919 (1971).

[12]F. Hopkins, D. O. Elliott, C. P. Bhalla, and P. Richard, Phys. Rev. A 8, 2952 (1973).

Spatially Resolved and Stark-Broadened X-Ray Lines from Laser-Imploded Targets

B. Yaakobi and A. Nee
Laboratory for Laser Energetics, University of Rochester, Rochester, New York 14627
(Received 8 March 1976)

We report the first observation of spatially resolved x-ray lines from laser-irradiated spherical targets. The lines are found to emanate mainly from inside the critical layer but the density they all indicate is not much higher than critical. These results are relevant to the study of heat conductivity and the laser ponderomotive force.

The transfer of absorbed laser energy into super-critical layers of an irradiated target has been shown recently to be very complicated. In particular, heat flow may be inhibited by magnetic fields[1] or be nonclassical[2] and the density profile may be modified by the laser ponderomotive force.[3] We show here that x-ray-line spectroscopy with spatial resolution can be a very useful tool for studying such effects. The targets used in these experiments, spherical glass shells, contain a variety of species (silicon, oxygen, sodium, magnesium) and the comparison of their spectra forms the basis for the present method. Additional information was gained by comparing such measurements with the emission at twice the laser frequency, which was spatially[4] and temporally[5] resolved. The results indicate a plateau (or "upper shelf") in the density profile ex-

tending roughly 20–30 μm inwards from the critical layer (see Fig. 2). The failure to observe densities substantially higher than critical can be the result of reduced or inhibited heat conductivity.

A four-beam glass:Nd laser system producing pulses of length 0.2–0.4 nsec was used to illuminate spherical glass shells of diameter about 90 μm and wall thickness 1 μm. The fill gas was neon at about 10-atm. pressure. Absorbed energy from all four beams ranged from 5 to 10 J. Incident power was 0.6–0.8 TW and power density $(2-3)\times10^{15}$ W/cm^2. A more detailed description of the laser system and diagnostic methods employed can be found in the literature.[6] Spectra were analyzed by a flat thalium acid phthalate crystal and recorded on a calibrated no-screen film. A slit of width 14 μm was placed between the target and the (nonfocusing) spectrometer so as to achieve a linear magnification of 7 and a spatial resolution of 16 μm in a direction perpendicular to that of the spectral resolution.

The usefulness of the x-ray spectra lies in the fact that lines from a given species will be emitted mostly when the temperature lies in a certain limited range. By spatially resolving the strong resonance lines in heliumlike and hydrogenlike ions of the glass elements we can find the target regions where these species emit strongly. Using the spatially-integrated spectra we can then estimate the temperature and density at these respective regions. Figures 1 and 2 show that the emission from the various species comes from well-defined thin shells which are slightly displaced with respect to each other. This kind of characteristic behavior is expected, even though the spectra are time integrated. Thermal energy flows from the critical layer into the expanding glass shell in the form of a sharp heat step function of temperature ~1 keV.[7] Lines from light elements ($Z\lesssim12$) are thus emitted predominantly within the narrow heat front. Even as it moves in, the region emitting a given spectral line will approximately retain its temperature. Unless absorbed energy is too high, the heat-front movement is arrested by a rarefaction wave (ablation) and this gives rise to a quasistationary spatial profile. Since x-ray emission is weighted by the density, we expect most of the line radiation to come from the conduction layer and to be sensitive to the heat conductivity and the density profile behind the critical layer. Figure 1 shows that sodium resonance lines come from inside the critical layer. To see this we note that the criti-

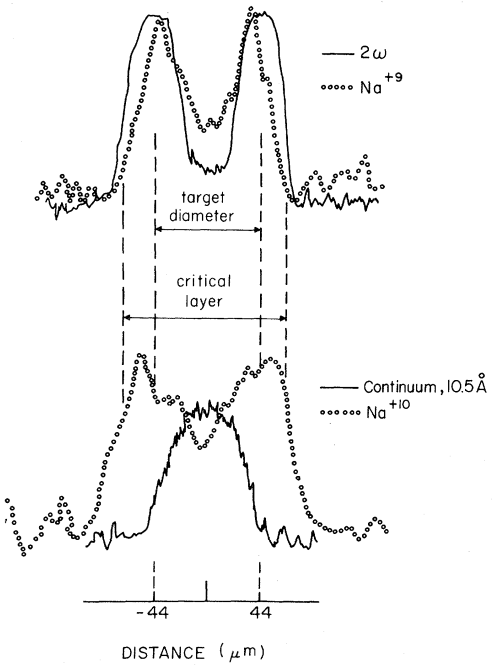

FIG. 1. Spatially resolved emissions of 2ω, twice the laser frequency (Ref. 4) (resolution 10 μm), the resonance lines of Na^{+9} and Na^{+10}, and a band of the continuum around 10.5 Å (resolution 16 μm). All intensities are in arbitrary units. Also shown are the original target position and the maximum excursion of the critical layer. The continuum was not employed in the present study.

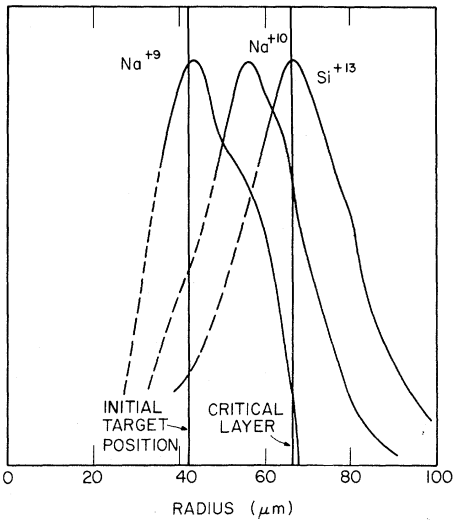

FIG. 2. Spatial distribution of some sodium and silicon resonance lines obtained by applying an Abel inversion program to results such as in Fig. 1. The plasma was assumed cylindrical. The inversion results inside the emitting shell are uncertain. The profile for Si^{+12} is similar to that of Si^{+13}

cal layer (as determined by the emission at twice the laser frequency) was found to spend most of the pulse duration at the position of its maximum excursion.[5] Also, it is the outer edge of the 2ω-emission contour which marks this position.[4] We see that species of lower charge are excited at smaller radii which is evidence of an inwardly decreasing temperature. The Abel inversion procedure required to derive Fig. 2 from results such as in Fig. 1 assumed the plasma to be cylindrical. This was found to be the case when imaging the target with an x-ray pinhole camera in and perpendicular to the plane of the laser beams.

We now turn to the spatially integrated spectra and give only a few examples of how they were used to derive temperature and density estimates. The temperature from the silicon spectrum (Fig. 3) was estimated using three intensity ratios: (a) between the resonance lines of Si^{+13} and Si^{+12}, (b) between the $1s^2$-$1s3p$ and $1s^2$-$1s2p$ lines of Si^{+12}, and (c) between the resonance line of Si^{+12} and the nearby group of dielectronic satellites.[8] We assume a steady-state corona model[9] in (a) but no such assumption is required in (b) or (c). Two conditions are required for the steady-state corona model to be valid: $N_e < 10^{16} z^7 (kT/I_z)^{1/2}$, where I_z is the ionization energy; also, the ionization time $\tau \sim 10^8 z^3/N_e$ (assuming $I_z/kT = 2.5$) should be shorter than plasma characteristic

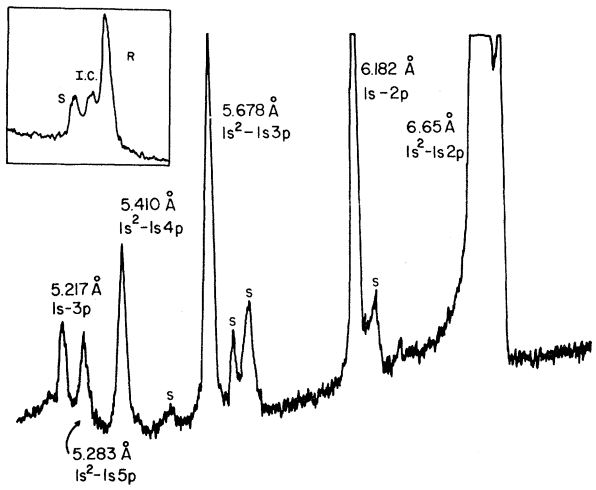

FIG. 3. Part of the silicon x-ray spectrum. The sharp cut on the right corresponds to the edge of the crystal. Note the well-resolved dielectronic satellites (marked s) and the new satellite at 5.561 ± 0.008 Å. Inset: R, the resonance line is $1s^2$-$1s2p^1P$ at 6.65 Å; I.C., the intercombination line $1s^2$-$1s2p^3P$ at 6.69 Å; S, dielectronic satellites [designated (Ref. 8) j,k,l] around 6.73 Å.

times. Density estimates below show the first condition to be satisfied here. Ionization times vary from about 50 to 200 psec when z increases from 8 to 13. The distance ions travel during this time is not much larger than the resolution length in Fig. 2. We conclude that steady state is marginally applicable, especially since the ratio (a) is extremely sensitive to T. In fact, if we solve the coupled equations which describe the steady-state corona model for the silicon ions we find that Si^{+12} attains its maximum abundance at 0.8 keV and Si^{+13} at 1 keV; the observed ratio (a) is that predicted by this model for $T = 0.9$ keV. A similar situation is found for the other species. The ratios (b) and (c) are inconsistent with this result and can only be understood if resonance lines are attenuated by absorption. If we assume the resonance line of Si^{+12} to be attenuated by a factor of 3, then *both* ratios (b) and (c) give approximately $T = 0.9$ keV. This attenuation can be shown to be consistent[10] with the product of density and plasma shell thickness as discussed below. A reduction by a factor of 3 in the intensity ratio (a) results in a reduction of only 20% in T. Actually, the resonance line of Si^{+13} should also be slightly absorbed and the error could be somewhat smaller. Comparing these and similar results we conclude that the temperature drops from about 0.9 keV around the critical layer (peak radiation of silicon) to about 150 eV (peak radiation of oxygen) over a distance which we can only roughly estimate as 20–30 μm.

The density is estimated by two methods. First, the intensity ratio between the resonance line $1s^2$-$1s2p^1P$ and the intercombination line $1s^2$-$1s2p^3P$ is weakly dependent on temperature and increases linearly with N_e when the quenching rate of the metastable state is intermediate to the radiative decay rates of the singlet and triplet states.[11] Accounting for self-absorption of the resonance line as above gives an observed ratio of about 10 for silicon (Fig. 3, inset). The corresponding density is about equal to the critical density $N_c = 10^{21}$ cm^{-3}, in agreement with Fig. 2. We have assumed here $T = 0.9$ keV; varying T by a factor of 2 will only change the derived value of N_e by about 30%. The intercombination lines in the lower-Z spectra should be weaker even for the same density and were hardly discernible in our spectra.

We finally estimate the density from the Stark widths of the last resolvable lines in the various resonance series. These lines would be broadened predominantly by ions which can be treated

in the quasistatic approximation and the high-lying levels would be hydrogenic (degenerate) even for the heliumlike ions. We note that for a given N_e the broadening due to ions decreases with z like $z^{-2/3}$ whereas the broadening due to electrons decreases like z^{-3} (assuming a constant T/z^2). We forego at this stage accurate profile calculations and seek only the line half-widths. The quasistatic Holtsmark broadening in angular frequency units of a transition from level n_i to n_f in an ion of charge z due to ions of density N_p and charge z_p is[12] $\Delta\omega = (12 z_p h/zm)(n_i^2 - n_f^2) N_0^{2/3}$. To account for ion-ion correlation we divide this expression by the ratio of the linewidth due to a Holtsmark distribution and that due to a correlated distribution.[13] The appropriate value of z in these calculations enter only in the Holtsmark "normal" field[13] and in the Debye length. For oxygen, this length turns out to be slightly smaller than the interparticle distance and we must extrapolate Hooper's results.[13] The same procedure in equivalent low-z cases[12] has a precision better than a factor of 2, but the precision for the spectra under discussion is not really known. The silicon lines (Fig. 3) are broadened mostly due to the finite size of the emitting plasma. Even for the last resolvable line of the $1s^2$-$1snp$ series (i.e., $n = 5$) we see no further broadening with respect to earlier series members and this translates into $N_e \ll 5N_c$. Oxygen lines from high-lying levels (more sensitive to the Stark effect because of the lower z) do show a significant Stark broadening (Fig. 4). Assuming Voigt profiles and eliminating the instrumental broadening (given by the narrowest line in the spectrum) we obtain for the lines $1s$-np ($n = 5$, 6, 7) the widths 16, 19, and 31 mÅ; the last width was derived from the long-wavelength wing of the line. The first and third of these give a density of $N_e \sim N_c$; the $1s$-$6p$ line appears too narrow for this density, probably because of its unshifted Stark component. The highest transition in sodium which is clearly seen is $1s^2$-$1s4p$ which barely shows a broadening beyond the instrumental width. This translates into $N_e \ll 6N_c$.

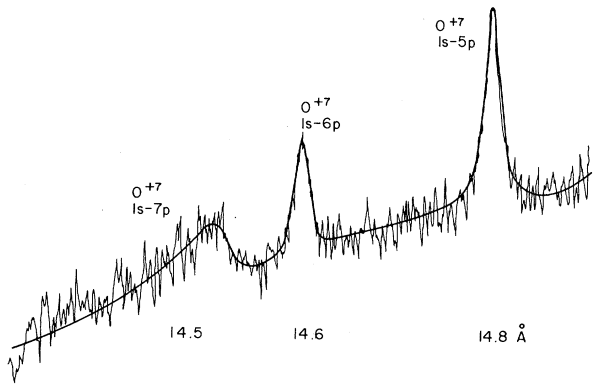

FIG. 4. The last few resolvable lines of H-like oxygen.

Two important conclusions seem to follow from these measurements. First, by comparing the density obtained by the various species and from Figs. 1 and 2, it follows that a region of thickness $\lesssim 20$–30 μm behind the critical layer has a density confined to the approximate range (1–2)N_c. This could be an observation of the "upper shelf" seen in particle simulations.[3] It follows from here that the pressure in the conduction region increases outwards which resembles the choked flow through a nozzle (the sonic point would be close to the critical layer). Second, the penetration depth of the heat front from the critical layer inwards is given approximately by[7] $d \sim K/vN_e$ where K is the heat conductivity and v the ion thermal speed. For $d \sim 20$ μm one calculates a value of N_e an order of magnitude larger than actually measured. This can be explained by a coefficient K an order of magnitude smaller than classical which prevents the heat front from penetrating into the denser part of the expanded glass shell.

We are grateful to L. M. Goldman, T. C. Bristow, J. Hoose, and S. Letzring for fruitful discussions and invaluable assistance. This work was supported by the Laser Fusion Feasibility Project in the Laboratory for Laser Energetics at the University of Rochester.

[1]B. H. Ripin *et al.*, Phys. Rev. Lett. 34, 1313 (1975).

[2]R. C. Malone, R. L. McCrory, and R. L. Morse, Phys. Rev. Lett. 34, 721 (1975); W. C. Mead, W. L. Kruer, J. D. Lindl, and H. D. Shay, Lawrence Livermore Laboratory Report No. 77, 1975 (to be published), p. 139.

[3]J. M. Kindel, Bull. Am. Phys. Soc. 20, 1230 (1975); D. W. Forslund *et al.*, Phys. Rev. A 11, 679 (1975), and Phys. Rev. Lett. 36, 35 (1976); J. S. DeGroot and J. E. Tull, Phys. Fluids 18, 672 (1975).

[4]S. Jackel, J. Albritton, and E. B. Goldman, Phys. Rev. Lett. 35, 514 (1975).

[5]S. Jackel, J. Albritton, E. B. Goldman, and S. Letzring, Bull. Am. Phys. Soc. 20, 1335 (1975).

[6]J. Soures, L. M. Goldman, and M. Lubin, Nucl. Fusion 13, 829 (1973).

[7]K. A. Brueckner and S. Jorna, Rev. Mod. Phys. 46, 325 (1974); K. A. Brueckner, R. A. Campbell, and

R. A. Grandey, Nucl. Fusion 15, 471 (1975).
[8]A. H. Gabriel, Mon. Not. Roy. Astron. Soc. 160, 99 (1972); C. P. Bhalla, A. H. Gabriel, and L. P. Presnyakov, Mon. Not. Roy. Astron. Soc. 172, 359 (1975).
[9]H. R. Griem, *Plasma Spectroscopy* (McGraw-Hill, New York, 1964), Chap. 6.
[10]A. G. Hearn, Proc. Phys. Soc., London 81, 648 (1963).
[11]A. H. Gabriel and C. Jordan, in *Case Studies in Atomic Collision Physics 2*, edited by E. W. McDaniel and M. R. C. McDowell (North-Holland, Amsterdam, 1972), Chap. 4.
[12]H. R. Griem, *Spectral Line Broadening by Plasmas* (Academic, New York, 1975), p. 8.
[13]C. F. Hooper, Phys. Rev. 165, 215 (1968); J. T. O'Brien and C. F. Hooper, Phys. Rev. A 5, 867 (1972).

Separated Local Field Spectra in NMR: Determination of Structure of Solids*

R. K. Hester, J. L. Ackerman, B. L. Neff, and J. S. Waugh
Department of Chemistry, Massachusetts Institute of Technology, Cambridge, Massachusetts 02139
(Received 15 March 1976)

Various techniques of coherent averaging in NMR are applied in time sequence and the transient signal is doubly Fourier analyzed. The result is a two-dimensional NMR spectrum in which dipole-dipole spectra of spins having slightly different chemical shifts are separated from one another. The results are useful for determination of atomic positions in solids.

We report here the experimental demonstration of an NMR technique which may be generally useful in the determination of atomic positions in solids.[1] It has long been known that such information resides in the nuclear magnetic dipole-dipole interactions. While in liquids these interactions are motionally averaged to zero, there are so many such couplings in solids that the NMR spectrum, except in a few special cases,[2] has an unresolvable "wide-line" character. In principle the structural information is extractable via moment analysis,[3] but the difficulties, both experimental and theoretical, of obtaining higher-order moments preclude the application of this method to most solids.

We consider the spectrum of relatively dilute spins S which are coupled to abundant neighboring spins I through the interaction

$$\mathcal{H}_{IS} = -2\sum_n \sum_k b_{nk} S_{zk} I_{zk}, \tag{1}$$

where $b_{nk} = \gamma_S \gamma_I \hbar r_{nk}^{-3} P_2(\cos\theta_{nk})$ contains the structural information. The I spins, because they are abundant, interact among themselves through

$$\mathcal{H}_{II} = \sum_l \sum_{k<l} b_{kl} (\vec{I}_k \cdot \vec{I}_l - 3 I_{zk} I_{zl}). \tag{2}$$

In addition the S spins have chemical shifts Δ_n which might be resolvable in the absence of I-S dipolar broadening[4]:

$$\mathcal{H}_{\Delta S} = \sum_n \Delta_n S_n. \tag{3}$$

Now we imagine giving the S spins an initial transverse polarization $\langle S_+(0)\rangle = \langle S_x\rangle + i\langle S_y\rangle$ at time zero which is then allowed to decay in two stages. In the first time interval, t_1, a line-narrowing irradiation is applied to the I spins resulting in a suppression of $\mathcal{H}_{II}$ and in a scaling of $\mathcal{H}_{IS}$ by a factor κ.[5] Then $\mathcal{H}_{IS}$ is suppressed in the second time interval, t_2, by strong resonant irradiation of the I spins while the remainder of the S free induction decay is recorded.[4] The signal observed at $t_1 + t_2$ has the form

$$\langle S_+(t_1,t_2)\rangle = \langle \exp[i(\mathcal{H}_{\Delta S} + \kappa\mathcal{H}_{IS})t_1] \exp(i\mathcal{H}_{\Delta S} t_2) S_+ \exp(-i\mathcal{H}_{\Delta S} t_2) \exp[-i(\mathcal{H}_{\Delta S} + \kappa\mathcal{H}_{IS})t_1]\rangle. \tag{4}$$

Making use of $S_+ = \sum_n S_{+n}$ and the local-field form of $\mathcal{H}_{\Delta S}$ and $\mathcal{H}_{IS}$, Eq. (4) is readily simplified to

$$g(t_1,t_2) \equiv \langle S_+(t_1,t_2)\rangle / \langle S_+(0,0)\rangle = \sum_n \exp\{i[\Delta_n t_2 + (\Delta_n + D_n)t_1]\} \tag{5}$$

with $D_n = -2\kappa\sum_k b_{nk} m_k$, where m_k is the magnetic quantum number of the kth neighboring I spin of S_n.

A Fourier analysis of $g(0,t_2)$ with respect to t_2 gives the pure chemical-shift spectrum $f(\omega_2)$ of the S system[4]; a similar analysis of $g(t_1,0)$ with respect to t_1 yields a sort of "wide-line" spectrum, $f(\omega_1)$, from which the effects of the I-I interactions have been removed. Two-dimensional Fourier analysis[6]